Asian J Biol Life Sci., 2026; 15(1):173-192.
https://ajbls.com

Research Article

In silico Design and Molecular Docking Evaluation of Phenothiazine Derivatives as Selective Celecoxib Bound to S121P Murine COX-2 Inhibitors for Targeted Therapy of Inflammatory Bowel Disease

Mayuri Girish Dharam[1], Rohit Jaysing Bhor[1,*], Mahesh Hari Kolhe[1], Mayuri Rajesh Bhoknal[2], Pratibha Shankar Jadhav[2]

[1]Department of Pharmaceutical Chemistry, Pravara Rural College of Pharmacy, Pravaranagar, Rahata, Ahmednagar, Maharashtra, INDIA.
[2]Department of QA, Pravara Rural College of Pharmacy, Pravaranagar, Rahata, Ahmednagar, Maharashtra, INDIA.

ABSTRACT

Introduction: Inflammatory Bowel Disease (IBD), encompassing Crohn's disease and ulcerative colitis, is a chronic inflammatory condition characterized by dysregulated immune responses and excessive production of pro-inflammatory mediators. Despite advancements in therapeutic strategies, current treatments are often associated with limitations such as adverse effects, high cost, and reduced long-term efficacy. Therefore, the identification of novel, safe, and effective therapeutic agents remains a significant challenge. **Materials and Methods:** In the present study, a series of phenothiazine-based derivatives (MD-1 to MD-12) were designed and evaluated using an integrated *in silico* approach. The crystal structure of Cyclooxygenase-2 (COX-2) (PDB ID: 5JW1) was selected as the target protein due to its critical role in mediating inflammatory responses. Molecular docking analysis was performed to assess the binding affinity and interaction patterns of the designed compounds within the active site of COX-2. **Results:** The docking results revealed that several derivatives, particularly MD-5, MD-6, MD-7, and MD-8, exhibited strong binding affinities with docking scores ranging from −10.0 to −10.4 kcal/mol, along with stable hydrogen bonding, electrostatic, and hydrophobic interactions. Furthermore, physicochemical properties, pharmacokinetic behavior, and drug-likeness of the compounds were evaluated using established computational tools. Most derivatives demonstrated favorable oral bioavailability, acceptable lipophilicity, optimal topological polar surface area, and compliance with Lipinski's rule of five. ADME analysis indicated high gastrointestinal absorption and minimal blood-brain barrier permeability, suggesting reduced central nervous system side effects. **Conclusion:** These compounds may serve as potential lead molecules for further experimental validation and development of targeted therapies for IBD.

Keywords: ADME Analysis, Anti-inflammatory Agents, Cyclooxygenase-2 (COX-2), Inflammatory Bowel Disease (IBD), Molecular Docking, Phenothiazine Derivatives, Structure-Based Drug Design.

Correspondence:
Dr. Rohit Jaysing Bhor
Department of Pharmaceutical Chemistry, Pravara Rural College of Pharmacy, Pravaranagar, Rahata, Ahmednagar, Maharashtra, INDIA.
Email: rohit.bhor69@gmail.com
ORCID: 0000-0002-7979-3765

Received: 04-02-2026;
Revised: 18-03-2026;
Accepted: 28-04-2026.

INTRODUCTION

Inflammatory Bowel Disease (IBD) is a chronic, immune-mediated disorder of the gastrointestinal tract, primarily comprising Crohn's disease and Ulcerative colitis (Abraham *et al*., 2009). Both conditions are characterized by relapsing intestinal inflammation resulting from an exaggerated immune response toward gut microbiota in genetically predisposed individuals (Barnes *et al*., 2011). The global incidence of IBD has increased steadily over recent decades, particularly in developing nations, reflecting the influence of environmental and lifestyle factors on disease progression (Baumgart *et al*., 2012). Crohn's disease may involve any part of the gastrointestinal tract and is typically associated with transmural inflammation and skip lesions (Chen *et al*., 1994). In contrast, ulcerative colitis is confined to the colon and rectum and presents with continuous mucosal inflammation. Despite differences in anatomical distribution and pathological features, both diseases share common molecular mechanisms involving cytokine dysregulation and activation of inflammatory signaling pathways. Molecular Pathogenesis of IBD (Daina *et al*., 2017). The pathophysiology of IBD is multifactorial and involves complex interactions among genetic susceptibility, microbial imbalance, epithelial barrier dysfunction, and immune

OPEN ACCESS

Manuscript TECHNOMEDIA

DOI: 10.5530/ajbls.20260133

system hyperactivation (Danese *et al*., 2011). Central to disease progression is the overproduction of pro-inflammatory cytokines such as Tumor Necrosis Factor alpha (TNF-α), Interleukin-6 (IL-6), and Interleukin-23 (IL-23) (DiMasi *et al*., 2016). These mediators activate transcription factors including Nuclear Factor kappa B (NF-κB), which regulates genes responsible for inflammation, immune cell recruitment, and tissue injury. Additionally, intracellular signaling pathways such as the Janus Kinase 1 (JAK1)-STAT axis contribute to cytokine-driven immune responses (Egan *et al*., 2000). Persistent activation of these pathways results in epithelial damage, ulcer formation, and chronic intestinal inflammation (Ghose *et al*., 1999). Therapeutic management of IBD includes aminosalicylates, corticosteroids, immunomodulators, and biologic agents targeting TNF-α and interleukin pathways (Kaplan *et al*., 2015). While biologics have improved remission rates, several challenges remain, including high treatment costs, adverse effects, immunogenicity, and loss of therapeutic response over time (Kitchen *et al*., 2004). These limitations highlight the necessity for novel, targeted, and cost-effective therapeutic strategies. Recent computational studies have screened phytochemicals, flavonoids, alkaloids, and synthetic derivatives against TNF-α, NF-κB, and JAK1 proteins (Lionta *et al*., 2014). Compounds exhibiting favorable binding affinities and stable interaction profiles are further subjected to molecular dynamics simulations and ADMET analysis to evaluate pharmacokinetic and toxicity parameters. Docking-assisted drug discovery accelerates the identification of anti-inflammatory agents capable of modulating cytokine release, inhibiting transcription factor activation, and suppressing downstream inflammatory cascades (Lipinski *et al*., 2004). This approach significantly reduces laboratory workload and improves cost-efficiency during early-stage drug development. Inflammatory bowel disease is driven by immune dysregulation and excessive cytokine-mediated inflammation involving TNF-α, IL-6, IL-23, NF-κB, and JAK-STAT signaling pathways (Meng *et al*., 2011). Although current therapies provide symptomatic relief, their limitations necessitate innovative treatment strategies (Morris *et al*., 2008). Molecular docking serves as a powerful computational tool for identifying and optimizing novel inhibitors targeting key inflammatory mediators in IBD. Integration of in silico modeling with experimental validation holds promise for the development of safer, targeted, and more effective therapeutics for long-term disease management (Muegge *et al*., 2003).

Molecular Targets in Docking Studies for Inflammatory Bowel Disease (IBD) and their Mechanistic Role

Inflammatory Bowel Disease (IBD), comprising Crohn's disease and Ulcerative colitis, is driven by persistent activation of immune and inflammatory signaling pathways within the intestinal mucosa. Molecular docking studies in IBD primarily focus on key regulatory proteins that orchestrate cytokine production, immune cell differentiation, and transcriptional control of inflammatory genes (Neurath *et al*., 2014). One of the principal targets in docking investigations is Tumour Necrosis Factor alpha (TNF-α), a pro-inflammatory cytokine that plays a central role in amplifying intestinal inflammation (Pires *et al*., 2015). TNF-α binds to its membrane receptors and activates downstream signaling cascades, including NF-κB and MAPK pathways, leading to increased expression of adhesion molecules, recruitment of inflammatory cells, and disruption of epithelial barrier integrity (Podolsky *et al*., 2002). Computational docking approaches aim to identify small molecules capable of interfering with TNF-α binding or destabilizing its active conformation, thereby attenuating cytokine-mediated inflammatory responses (Pushpakom *et al*., 2019). Another critical molecular target is Nuclear Factor kappa B (NF-κB), a transcription factor that regulates genes encoding cytokines, chemokines, and other inflammatory mediators (Ricciotti *et al*., 2011). In IBD, persistent activation of NF-κB results from cytokine stimulation and degradation of its inhibitory proteins, enabling its translocation into the nucleus where it promotes sustained inflammatory gene expression (Sliwoski *et al*., 2014). Docking studies often focus on inhibiting the DNA-binding domain of NF-κB or targeting upstream kinases responsible for its activation, with the goal of suppressing transcriptional amplification of inflammation. The Janus Kinase 1 (JAK1) enzyme is also widely investigated in structure-based drug design for IBD (Torres *et al*., 2017). JAK1 participates in the JAK-STAT signaling pathway, which is activated by multiple interleukins implicated in intestinal inflammation. Upon cytokine receptor engagement, JAK1 phosphorylates STAT proteins, promoting their nuclear translocation and transcriptional activation of immune-related genes (Trott *et al*., 2010). Molecular docking strategies targeting the ATP-binding site of JAK1 aim to inhibit its kinase activity, thereby reducing cytokine-driven immune activation and inflammatory progression. In addition, the Interleukin-23 Receptor (IL-23R) represents a significant target due to its involvement in the IL-23/Th17 axis. Activation of this receptor promotes differentiation and maintenance of Th17 cells, which secrete pro-inflammatory cytokines that contribute to chronic intestinal inflammation. Docking studies seek to block ligand-receptor interactions or disrupt associated signaling mechanisms to attenuate Th17-mediated immune responses. Another important enzyme frequently evaluated in docking studies is Cyclooxygenase-2 (COX-2) (Vane *et al*., 1998). Overexpression of COX-2 in inflamed intestinal tissues leads to elevated prostaglandin production, enhancing vascular permeability, edema, and pain. Structure-based inhibition of COX-2 through molecular docking focuses on compounds capable of occupying its catalytic hydrophobic channel and preventing prostaglandin synthesis. Collectively, these molecular targets represent critical nodes in the inflammatory network underlying IBD pathogenesis (Veber *et al*., 2002). By computationally predicting ligand-protein interactions

and binding affinities, molecular docking provides a rational framework for identifying novel small-molecule inhibitors that can modulate cytokine signaling, transcriptional regulation, and enzymatic pathways involved in intestinal inflammation (Wallace *et al.*, 2008). Such structure-guided approaches significantly contribute to the development of targeted and potentially safer therapeutic strategies for long-term management of IBD.

MATERIALS AND METHODS

Target Proteins Selection

The crystal structure with PDB ID 5JW1 represents the selective COX-2 inhibitor celecoxib bound to a mutant form of murine cyclooxygenase-2 in which serine at position 121 is Substituted with Proline (S121P). This structure provides detailed insight into the molecular basis of selective COX-2 inhibition and is widely used in structure-based drug design studies. Cyclooxygenase-2, formally known as Cyclooxygenase-2 (COX-2), is an inducible enzyme responsible for converting arachidonic acid into prostaglandins during inflammation. Overexpression of COX-2 is strongly associated with inflammatory disorders, including Inflammatory bowel disease, rheumatoid arthritis, and colorectal cancer. Selective inhibition of COX-2 reduces prostaglandin-mediated inflammation while minimizing gastrointestinal side effects typically associated with COX-1 inhibition. In the 5JW1 structure, celecoxib occupies the long hydrophobic channel of the COX-2 catalytic site. The sulfonamide moiety of celecoxib extends into a secondary side pocket that is characteristic of COX-2 and absent in COX-1 (Warner *et al.*, 2004). This structural difference explains the drug's high selectivity. Key interactions within the active site include hydrophobic contacts with residues lining the channel and hydrogen bonding interactions involving the sulfonamide group and polar amino acids in the side pocket region. The binding conformation stabilizes the inhibitor within the cyclooxygenase active site, preventing arachidonic acid access and thereby blocking prostaglandin synthesis. The S121P mutation is located away from the catalytic channel and is generally introduced to enhance protein stability or crystallization efficiency without significantly altering inhibitor binding geometry (Wishart *et al.*, 2016). Structural comparisons indicate that celecoxib maintains a binding orientation consistent with previously reported COX-2-celecoxib complexes, supporting the reliability of this mutant structure for docking validation. The protein was provided in Figure 1 by the RCSB Protein Data Bank with https://www.rcsb.org/structure/5JW1.

Preparation of ligand

Phenothiazine and its substituted scaffolds were used as ligands for the docking study in Table 1. For chemical structures, Chem Draw was used to sketch, which were then converted into three-dimensional structures. Ligands were prepared by using Biovia Discovery Studio and Pyrex software. In structure-based drug design, computational tools play a central role in predicting ligand-protein interactions and evaluating binding affinity. Among the widely used platforms for molecular docking and interaction analysis are BIOVIA Discovery Studio and PyRx. These programs are frequently employed in pharmacological research, including studies targeting inflammatory mediators such as COX-2, TNF-α, and JAK1 in Inflammatory Bowel Disease (IBD). PyRx is an open-source virtual screening tool that integrates Auto-Dock and Auto-Dock Vina engines into a user-friendly graphical interface. It is widely applied in academic research due to its accessibility and efficiency in handling multiple ligands simultaneously. In many research workflows, PyRx is employed for docking simulations and calculation of binding energies, while Discovery Studio is used for detailed visualization and interaction profiling of the best-scoring ligand-protein complexes (Xavier *et al.*, 2007). This combined approach enhances reliability and clarity in reporting docking results. BIOVIA Discovery Studio is a comprehensive molecular modeling and visualization suite developed by Dassault Systèmes. It provides advanced tools for protein preparation, ligand optimization, docking, pharmacophore modeling, and molecular interaction analysis.

RESULTS

Bioavailability Radar (Swiss-ADME Radar Chart)

The bioavailability radar chart generated using Swiss ADME provides a visual summary of the key physicochemical properties that influence the oral bioavailability of the designed molecule given in Table 2. The radar plot evaluates six important parameters: Lipophilicity (LIPO), Molecular Size (SIZE), Polarity (POLAR), Solubility (INSOLU), Flexibility (FLEX), and Saturation (INSATU). The optimal range for each property is represented by the pink shaded region, while the red polygon represents the calculated properties of the compound. In the presented radar chart, the compound shows acceptable lipophilicity, indicating a balanced hydrophilic-lipophilic nature that favors membrane permeability and absorption. The molecular size parameter also falls within the optimal region, suggesting that the compound has a suitable molecular weight for oral drug candidates. The polarity parameter, generally represented by the Topological Polar Surface Area (TPSA), lies within the recommended range, indicating favorable potential for intestinal absorption. The Solubility (INSOLU) parameter appears close to the optimal region, suggesting moderate aqueous solubility, which is important for proper dissolution and absorption in the gastrointestinal tract. However, the Saturation (INSATU) value extends slightly outside the optimal range, indicating a lower fraction of sp^3 hybridized carbons. Such a deviation is relatively common in aromatic drug-like molecules and does not necessarily hinder biological activity. The Flexibility (FLEX) parameter, which is related to the number of rotatable bonds, also remains within acceptable limits, suggesting that the molecule maintains a suitable balance between structural rigidity and flexibility. This balance is

Table 1: Phenothiazine Structure; its IUPAC Name; Mol. Weight and Smiles.

Code	Structure	Mol. Wt	Smiles
MD-1	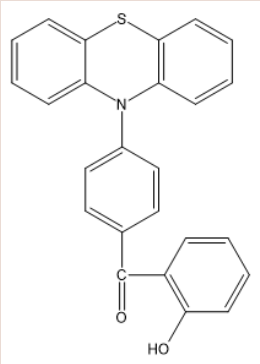	395.47gm/mol	O=C(C1=C(O)C=CC=C1)C(C=C2)=CC=C2N3C4=CC=CC=C4SC5=C3C=CC=C5
MD-2	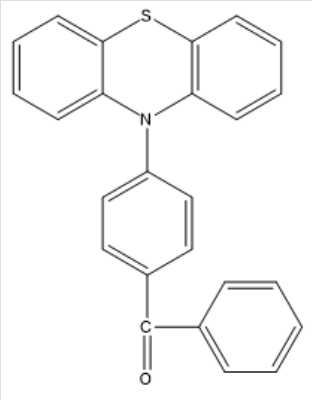	379.47gm/mol	O=C(C1=CC=CC=C1)C(C=C2)=CC=C2N3C4=CC=CC=C4SC5=C3C=CC=C5
MD-3	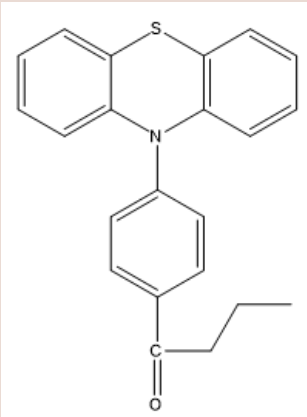	345.46gm/mol	O=C(CCC)C(C=C1)=CC=C1N2C3=CC=CC=C3SC4=C2C=CC=C4
MD-4	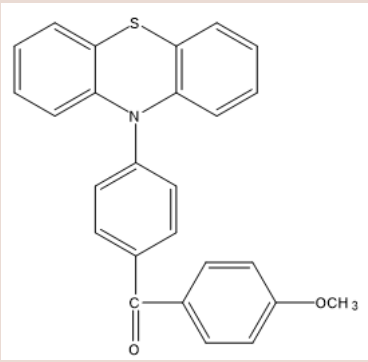	409.50gm/mol	O=C(C1=CC=C(OC)C=C1)C(C=C2)=CC=C2N3C4=CC=CC=C4SC5=C3C=CC=C5

MD-5	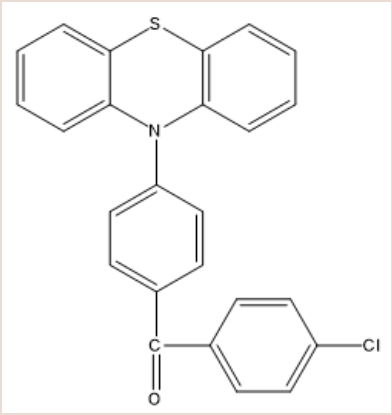	413.92 gm/mol	O=C(C1=CC=C(Cl)C=C1)C(C=C2)=CC=C2N3C4=CC=CC=C4SC5=C3C=CC=C5
MD-6	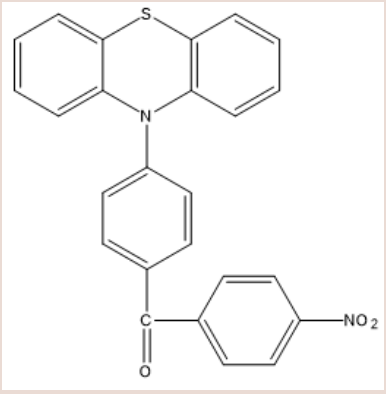	424.47 gm/mol	O=C(C1=CC=C([N+]([O])=O)C=C1)C(C=C2)=CC=C2N3C4=CC=CC=C4SC5=C3C=CC=C5
MD-7	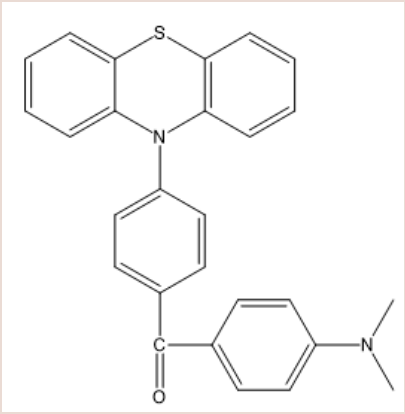	422.54 gm/mol	O=C(C1=CC=C(N(C)C)C=C1)C(C=C2)=CC=C2N3C4=CC=CC=C4SC5=C3C=CC=C5
MD-8	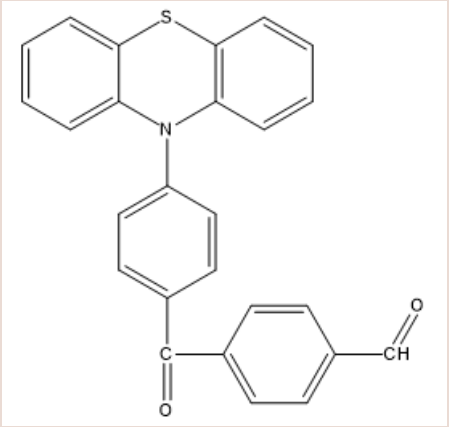	407.48 gm/mol	O=C(C1=CC=C(C=O)C=C1)C(C=C2)=CC=C2N3C4=CC=CC=C4SC5=C3C=CC=C5

MD9	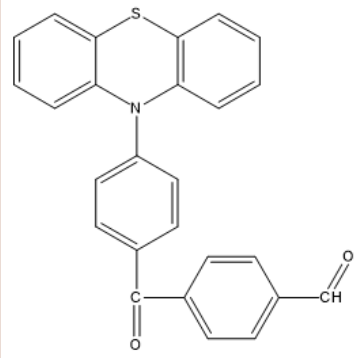	407.48	O=C(C1=CC=C(C=O)C=C1)C(C=C2)=CC=C2N3C4=CC=CC=C4SC5=C3C=CC=C5
MD10	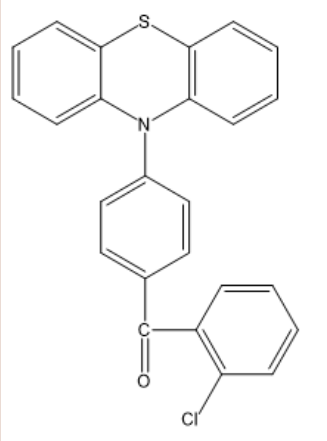	413.92	O=C(C1=C(Cl)C=CC=C1)C(C=C2)=CC=C2N3C4=CC=CC=C4SC5=C3C=CC=C5
MD11	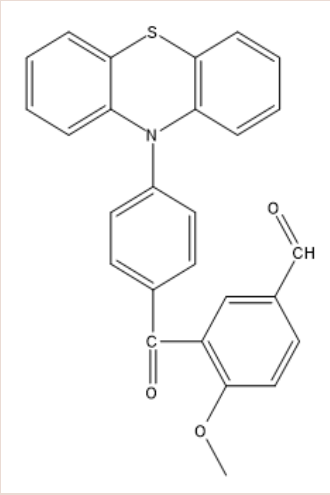	437.51	O=C(C1=C(OC)C=CC(C=O)=C1)C(C=C2)=CC=C2N3C4=CC=CC=C4SC5=C3C=CC=C5
MD12	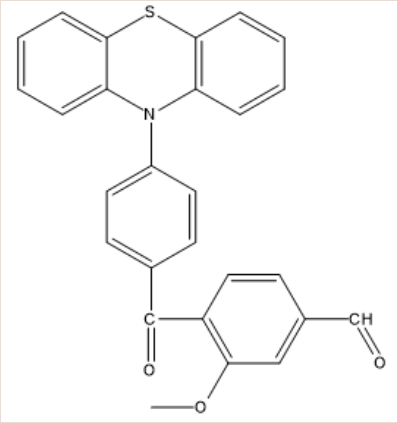	437.51	O=C(C1=C(OC)C=C(C=O)C=C1)C(C=C2)=CC=C2N3C4=CC=CC=C4SC5=C3C=CC=C5

important for maintaining proper binding orientation within the receptor binding pocket.

Interaction Analysis of Designed Molecules

The molecular docking study was performed to investigate the interaction pattern between the Designed Molecules (MD-1 to MD-12) and the active site residues of the target protein given in Table 3. The interaction analysis revealed that the ligands formed a variety of stabilizing interactions, including hydrogen bonds, electrostatic interactions, salt bridges, π-π stacking, π-alkyl interactions, and hydrophobic contacts. These interactions play an important role in stabilizing the ligand within the protein binding pocket and contribute to the overall binding affinity. Compound MD-1 exhibited a hydrogen bond interaction with GLY135 at a distance of approximately 2.47 Å, indicating strong binding stability. Additionally, electrostatic interactions with ASP157 were observed through π-anion and π-π T-shaped interactions, while several hydrophobic interactions involving residues such as TYR136, PRO156, PRO154, CYS36, and CYS47 further stabilized the ligand through π-alkyl interactions.

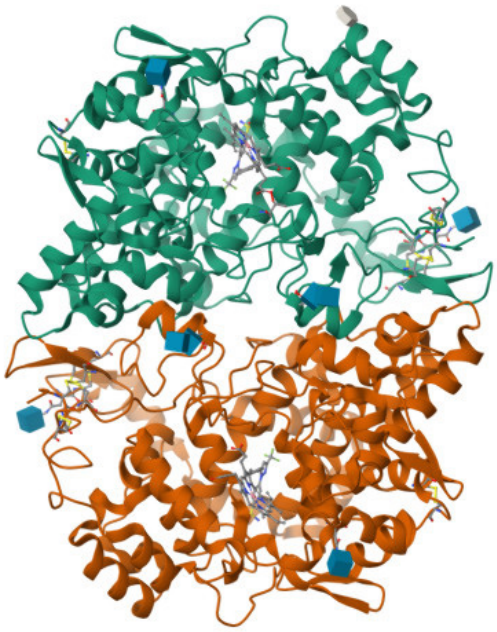

Figure 1: Crystal structure of Celecoxib bound to S121P murine COX-2 mutant| 5JW1 | pdb_00005jw1.

Similarly, MD-2 showed electrostatic interactions with ASP158 through π-anion interactions, while hydrophobic interaction with PRO156 via π-alkyl interaction contributed to ligand stabilization. An additional interaction with PHE52 involving π-sulfur interaction was also observed. Compound MD-3 demonstrated a strong binding pattern characterized by multiple salt bridge interactions with residues such as ARG44, ARG120, ARG184, LYS166, LYS211, ASP125, ASP499, ASP393, and GLU524. The interaction distances ranged from 1.77 Å to 2.70 Å, indicating strong electrostatic attraction and suggesting a highly stable ligand-protein complex. Compound MD-4 formed three hydrogen bonds with ARG376, ASN375, and GLY225, indicating strong polar interactions within the binding pocket. In addition, π-π T-shaped interactions with PHE142 and hydrophobic contacts with LEU145 and HIS226 contributed to the stabilization of the ligand. Compound MD-5 exhibited a hydrogen bond interaction with ARG376 at a distance of 2.02 Å. Multiple π-π T-shaped interactions with PHE142 and hydrophobic interaction with

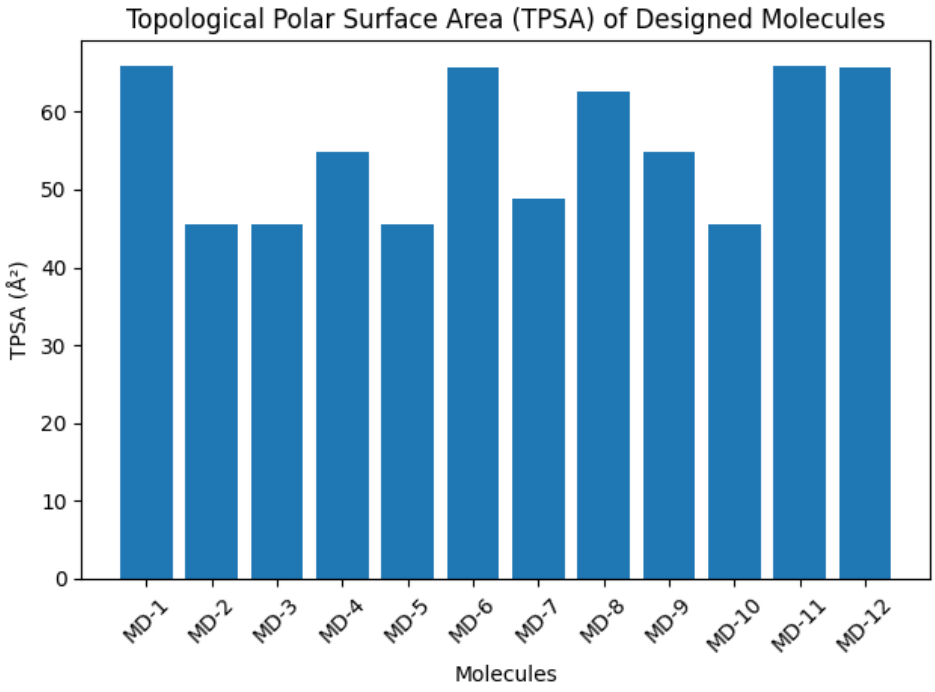

Figure 2: Topological Polar Surface Area (TPSA) of Design molecules MD1-MD12.

Table 2: The six parameters shown are shown as LIPO: Lipophilicity; SIZE: Molecular weight; POLAR: Polarity (TPSA); INSOLU: Insolubility; INSATU: Unsaturation; FLEX: Flexibilit.

Derivative Code	Radar chart (spider chart)	Derivative Code	Radar chart (spider chart)
MD-1	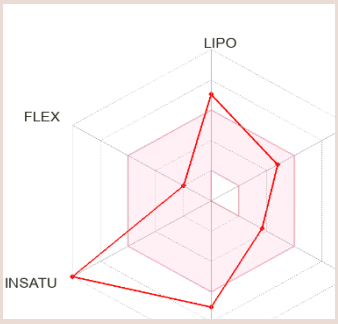	MD-2	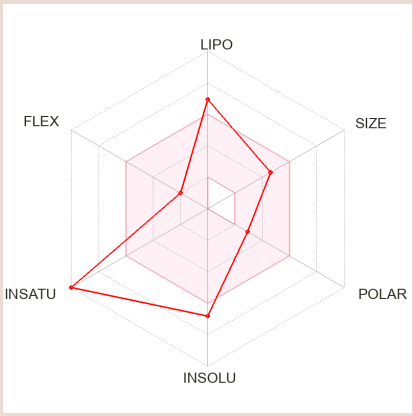
MD-3	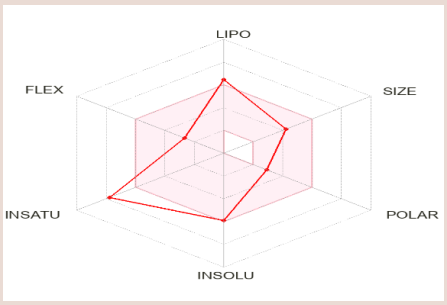	MD-4	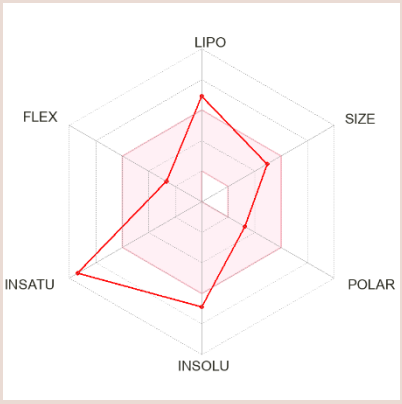
MD-5	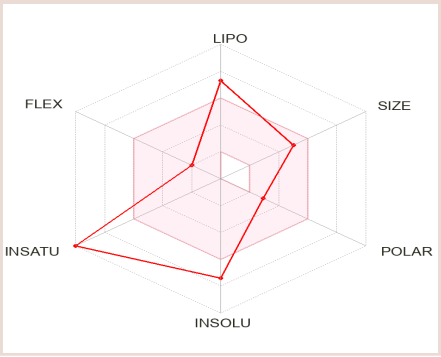	MD-6	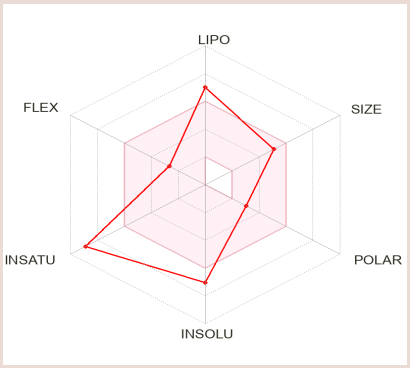
MD-7	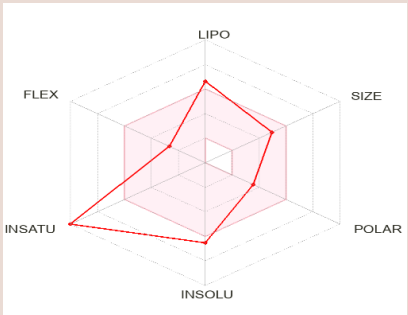	MD-8	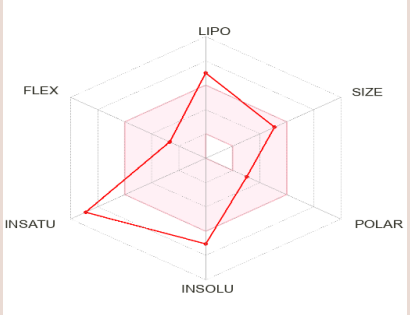

MD -9

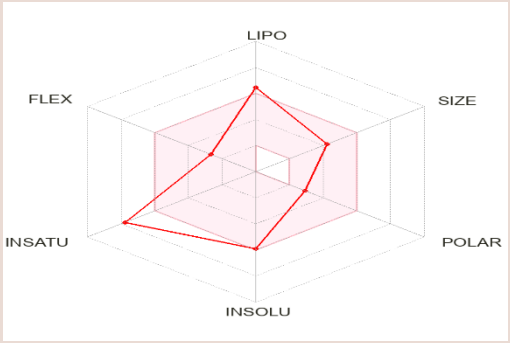

MD-10

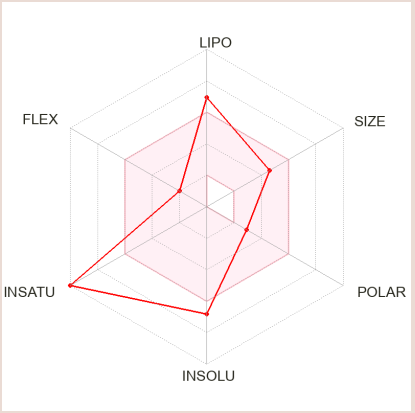

MD-11

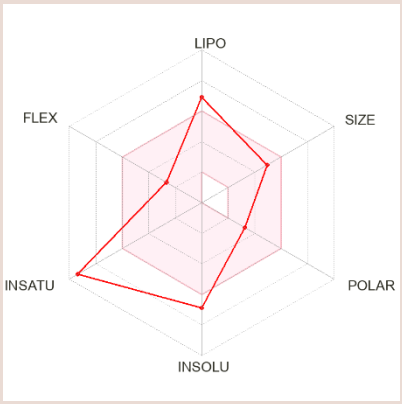

MD-12

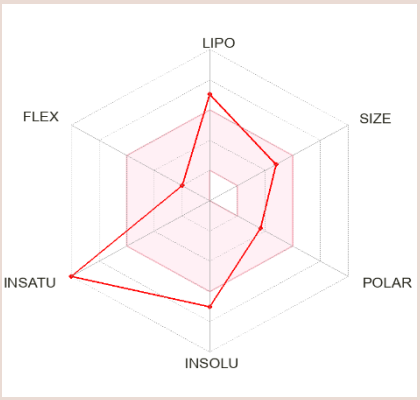

LEU145 further enhanced ligand stability. Compound MD-6 demonstrated three hydrogen bond interactions with ASN34, HIS39, and GLN461. Additionally, electrostatic interactions with ASP157 via π-anion interactions were observed. Hydrophobic interactions involving residues such as TYR136, PRO156, PRO154, CYS36, CYS47, and PRO153 further stabilized the ligand within the binding cavity. Similarly, MD-7 formed a hydrogen bond with ASN34, while electrostatic interactions with ASP157 were observed through π-anion interactions. Multiple hydrophobic interactions involving PRO153, PRO156, CYS47, CYS36, and PRO154 were also present, contributing to strong ligand binding. Compound MD-8 exhibited a hydrogen bond with ARG120 at 2.51 Å along with a π-cation electrostatic interaction with the same residue. Hydrophobic interactions with residues such as ILE112, TRP100, VAL89, LEU93, and VAL116 through π-alkyl and π-π T-shaped interactions further stabilized the ligand. Similarly, MD-9 displayed hydrogen bonding with ARG120 and several hydrophobic interactions involving TRP100, VAL89, LEU93, VAL116, and ILE112, indicating a stable binding configuration within the receptor binding pocket. Compound MD-10 formed a hydrogen bond with ASN34, while electrostatic interactions with ASP157 occurred through π-anion interactions. Hydrophobic interactions with TYR136, PRO156, PRO154, CYS36, and CYS47 contributed to the stabilization of the ligand-protein complex. Compound MD-11 demonstrated multiple hydrogen bond interactions with LYS83, ARG467, LYS473, and ASN43, suggesting strong polar interactions within the active site. Additionally, hydrophobic interactions involving PHE64, LEU80, PRO72, and LYS468 contributed to the stabilization of the ligand. Compound MD-12 formed hydrogen bonds with ARG44, while electrostatic interactions with LYS546 and ARG44 occurred through π-cation interactions. Hydrophobic contacts with PHE371, SER121, and ALA543 further contributed to ligand stabilization. Overall, the docking analysis revealed that the designed molecules formed multiple stabilizing interactions with key amino acid residues in the active site, including hydrogen bonds, electrostatic interactions, and hydrophobic contacts. Compounds such as MD-3, MD-6, MD-7, and MD-11 exhibited a higher number of strong interactions, suggesting improved binding stability and potential biological activity. These findings indicate that the designed molecules possess promising binding affinity toward the target protein and may serve as potential candidates for further pharmacological evaluation and drug development studies.

Comparative Analysis of Physicochemical and Drug-Likeness Properties

The physicochemical characteristics of the Designed Molecules (MD-1 to MD-12) were evaluated and given in Table 4 by using important parameters including the number of rotatable bonds, Hydrogen Bond Acceptors (HBA), Hydrogen Bond Donors (HBD), Molar Refractivity (MR), Topological Polar Surface Area (TPSA) graph given in Figure 2, and Lipophilicity indices

(iLOGP and XLOGP3). These parameters play a crucial role in determining the drug-likeness, membrane permeability, and oral bioavailability of potential therapeutic compounds. The number of rotatable bonds among the molecules ranged from 3 to 4, indicating moderate molecular flexibility. Compounds with fewer rotatable bonds generally exhibit improved conformational stability and better oral bioavailability. In this dataset, molecules such as MD-1, MD-2, MD-5, MD-10, and MD-11 possessed three rotatable bonds, while the remaining derivatives contained four rotatable bonds, suggesting acceptable flexibility within the limits recommended for drug-like molecules. The hydrogen bonding capacity, represented by hydrogen bond acceptors and donors, influences solubility and interactions with biological targets. The number of hydrogen bond acceptors ranged from 1 to 3, whereas hydrogen bond donors ranged from 0 to 1 across all derivatives. Molecules such as MD-6 and MD-12 exhibited the highest number of acceptors (3), which may enhance their ability to participate in intermolecular interactions with protein residues. In contrast, most derivatives lacked hydrogen bond donors, which may favor membrane permeability. The Molar Refractivity (MR) values varied between 107.99 and 132.26, reflecting differences in molecular size and polarizability. Compounds such as MD-7 showed relatively higher MR values, indicating increased molecular volume and electronic polarizability, which may influence binding interactions within the receptor active site. The Topological Polar Surface Area (TPSA) ranged from 45.61 to 65.84 Å², suggesting favorable absorption characteristics. Molecules with TPSA values below 140 Å² are generally associated with good intestinal absorption and potential blood-brain barrier permeability. In the present dataset, all compounds fall well within this acceptable range, indicating suitable polarity for drug development. Lipophilicity, represented by iLOGP and XLOGP3 values, is an essential parameter affecting membrane permeability and pharmacokinetic behavior. The iLOGP values ranged from 3.41 to 4.08, indicating moderate lipophilicity among the derivatives. Similarly, XLOGP3 values ranged between 5.82 and 7.28, suggesting that the compounds possess relatively hydrophobic characteristics that may enhance membrane penetration but require careful consideration to avoid excessive lipophilicity. Overall, the physicochemical evaluation indicates that all designed molecules exhibit acceptable drug-likeness characteristics, including appropriate molecular flexibility, balanced polarity, and moderate lipophilicity. These properties suggest that the compounds may possess favorable pharmacokinetic profiles and are suitable candidates for further molecular docking and biological activity evaluation.

Comparative Analysis of Pharmacokinetic and ADME Properties

The pharmacokinetic behavior of the Designed Molecules (MD-1 to MD-12) was assessed using important ADME parameters, including Gastrointestinal (GI) absorption, Blood-Brain Barrier (BBB) permeability, P-glycoprotein (P-gp) substrate status, cytochrome P450 enzyme inhibition, and skin permeability (log Kp) given in Table 5. These parameters are essential for evaluating the potential drug-likeness and metabolic behavior of candidate molecules. The gastrointestinal absorption results indicated that the majority of the compounds exhibited high GI absorption, suggesting favorable intestinal uptake and suitability for oral administration. Among the twelve derivatives, MD-5

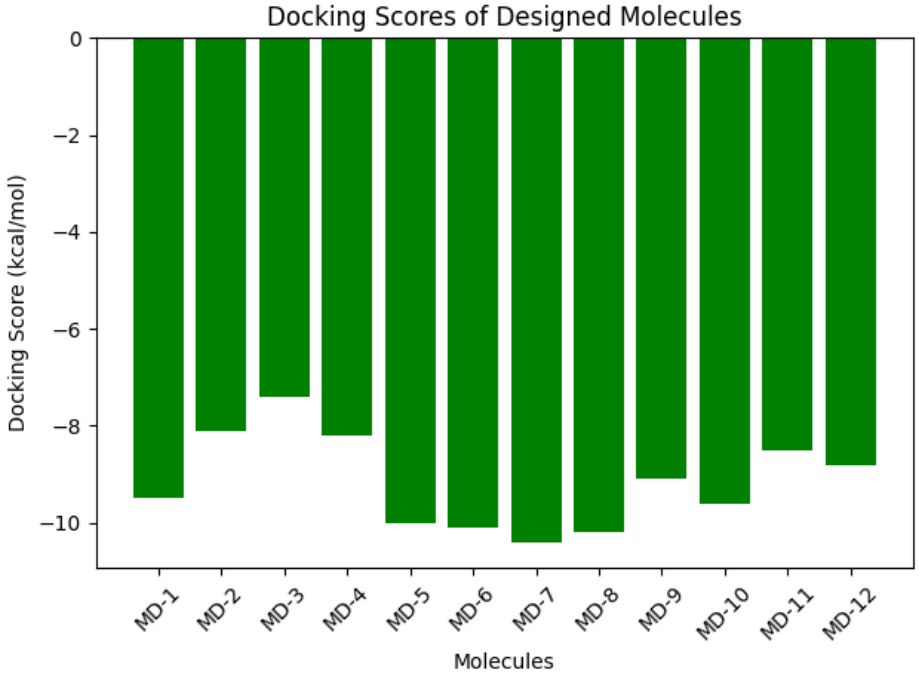

Figure 3: Molecular Docking Interaction Analysis.

and MD-12 showed low GI absorption, which may limit their oral bioavailability compared with the other compounds. The ability of compounds to cross the Blood-Brain Barrier (BBB) was also predicted. All molecules in the series were classified as non-BBB permeant, indicating limited penetration into the central nervous system. This property may be advantageous when the therapeutic target is located outside the brain, as it reduces the likelihood of central nervous system-related side effects. The P-glycoprotein (P-gp) substrate analysis revealed that most derivatives are predicted to be P-gp substrates, which means they may undergo active efflux by this transporter protein. However, MD-6 and MD-8 were identified as non-substrates,

Table 3: Multiple interactions involving different amino acids; Hydrogen Bond; Electrostatic and Hydrophobic interactions by MD -MD12 molecules.

Code	Name	Distance	Category	Type
MD-1	GLY135	2.47076	Hydrogen Bond	Pi-Anion
	ASP157	3.75183	Electrostatic	Pi-Pi T-shaped
	ASP157	3.43779	Electrostatic	Pi-Alkyl
	TYR136	5.10771	Hydrophobic	Pi-Alkyl
	PRO156	4.89841	Hydrophobic	Pi-Alkyl
	PRO154	4.93569	Hydrophobic	Pi-Alkyl
	CYS36	4.36695	Hydrophobic	Pi-Alkyl
	CYS47	4.98896	Hydrophobic	Pi-Alkyl
	PRO153	5.03502	Hydrophobic	
	PRO156	5.20444	Hydrophobic	
MD-2	ASP158	3.97621	Electrostatic	Pi-Anion
	ASP158	3.92977	Electrostatic	Pi-Anion
	PHE52	5.40761	Electroststic	Pi-Sulfur
	PRO156	5.05546	Hydrophobic	Pi-Alkyl
MD-3	ARG44	2.04788	Electrostatic	Salt Bridge
	ASP125	1.77062	Electrostatic Electrostatic	Salt Bridge
	ARG120	2.70548	Electrostatic	Salt Bridge
	GLU524	2.49218	Electrostatic	Salt Bridge
	ARG120	1.78166	Electrostatic	Salt Bridge
	GLU524	2.10194	Electrostatic	Salt Bridge
	LYS166	2.11852	Electrostatic Electrostatic	Salt Bridge
	ASP499	2.04656	Electrostatic	Salt Bridge
	ARG184	1.93583	Electrostatic	Salt Bridge
	ASP393	2.05942		Salt Bridge
	LYS211	2.20917		Salt Bridge
MD-4	ARG376	2.52858	Hydrogen Bond	Conventional
	ASN375	2.39231	Hydrogen Bond	Carbon Hydrogen Bond
	GLY225	3.66584	Hydrogen Bond	
	HIS226	3.56158	Hydrophobic	Pi-Pi T-shaped
	PHE142	4.93758	Hydrophobic	Pi-Pi T-shaped
	PHE142	5.10853	Hydrophobic	Pi-Pi T-shaped
	LEU145	4.85068	Hydrophobic	Pi-Alkyl
				Pi-Alkyl
MD-5	ARG376	2.02328	Hydrogen Bond	Conventional Hydrogen Bond
	PHE142	4.73284	Hydrophobic	Pi-Pi T-shaped
	PHE142	4.89607	Hydrophobic	Pi-Pi T-shaped
	PHE142	4.89785	Hydrophobic	Pi-Pi T-shaped
	LEU145	5.43213	Hydrophobic	Pi-Alkyl

MD-6	ASN34 HIS39 GLN461 ASP157 ASP157 TYR136 PRO156 PRO154 CYS36 CYS47 PRO153 PRO156	2.17574 2.12607 2.20179 3.72863 3.37958 5.13756 4.91784 5.18548 4.36348 5.08518 5.1669 4.81809	Hydrogen Bond Hydrogen Bond Hydrogen Bond Electrostatic Electrostatic Hydrophobic Hydrophobic Hydrophobic Hydrophobic Hydrophobic Hydrophobic Hydrophobic	Conventional Hydrogen Bond Conventional Hydrogen Bond Conventional Hydrogen Bond Pi-Anion Pi-Anion Pi-Pi T-shaped Pi-Alkyl Pi-Alkyl Pi-Alky
MD-7	ASN34 ASP157 ASP157 PRO153 CYS47 PRO153 HIS39 PRO156 PRO154 CYS36 CYS47 PRO153 PRO156	1.9424 3.4173 3.46315 4.34819 4.62394 4.35358 4.78116 4.96027 4.9329 4.4009 5.25025 5.44251 4.89522	Hydrogen Bond Electrostatic Electrostatic Hydrophobic Hydrophobic Hydrophobic Hydrophobic Hydrophobic Hydrophobic Hydrophobic Hydrophobic Hydrophobic Hydrophobic	Conventional Hydrogen Bond Pi-Anion Pi-Anion Alkyl Alkyl Alkyl Pi-Alkyl Pi-Alkyl Pi-Alkyl Pi-Alkyl Pi-Alkyl Pi-Alkyl
MD-8	ARG120 ARG120 ILE112 TRP100 VAL89 LEU93 VAL116 ILE112 ILE92 VAL89	2.51644 3.8255 2.52252 4.99984 5.28108 5.0775 5.4931 4.30429 5.12098 5.25738	Hydrogen Bond Electrostatic Hydrophobic Hydrophobic Hydrophobic Hydrophobic Hydrophobic Hydrophobic Hydrophobic Hydrophobic	Conventional Hydrogen Bond Pi-Cation Pi-Sigma Pi-Pi T-shaped Pi-Alkyl Pi-Alkyl Pi-Alkyl Pi-Alkyl Pi-Alkyl
MD-9	ARG120 ILE112 TRP100 VAL89 LEU93 VAL116 ILE112 ILE92 VAL89	2.52252 4.99984 5.28108 5.0775 5.4931 4.30429 5.12098 5.25738	Hydrogen Bond Electrostatic Hydrophobic Hydrophobic Hydrophobic Hydrophobic Hydrophobic Hydrophobic Hydrophobic	Conventional Hydrogen Bond Pi-Cation Pi-Sigma Pi-Pi T-shaped Pi-Alkyl Pi-Alkyl Pi-Alkyl Pi-Alkyl Pi-Alkyl

MD-10	ASN34 ASP157 TYR136 PRO156 PRO154 CYS36 CYS47 PRO153 PRO156	2.11478 3.73342 3.44158 5.18533 4.84738 5.00347 4.32525 4.92117 5.11313	Hydrogen Bond Electrostatic Electrostatic Hydrophobic Hydrophobic Hydrophobic Hydrophobic Hydrophobic Hydrophobic	Conventional Hydrogen Bond Pi-Anion Pi-Anion Pi-Pi T-shaped Pi-Alkyl Pi-Alkyl Pi-Alkyl Pi-Alkyl Pi-Alkyl
MD-11	LYS83 ARG467 ARG467 LYS473 ASN43 PHE64 PHE64 LEU80 LYS473 LYS468 PRO72 LEU80 LYS473	2.54245 2.68629 2.60073 2.1434 2.89471 5.42591 5.26972 5.07419 5.32209 5.23695 4.94362 5.45083 3.94697	Hydrogen Bond Hydrogen Bond Hydrogen Bond Hydrogen Bond Hydrogen Bond Hydrophobic Hydrophobic Hydrophobic Hydrophobic Hydrophobic Hydrophobic Hydrophobic Hydrophobic	Conventional Hydrogen Bond Conventional Hydrogen Bond Conventional Hydrogen Bond Conventional Hydrogen Bond Pi-Donor Hydrogen Bond Pi-Pi T-shaped Pi-Pi T-shaped
MD-12	ARG44 ARG44 LYS546 ARG44 PHE371 SER121 ALA543	2.32326 2.73387 4.62914 4.33678 5.32337 4.20064 4.9311	Hydrogen Bond Hydrogen Bond Electrostatic Electrostatic Hydrophobic Hydrophobic	Conventional Hydrogen Bond Conventional Hydrogen Bond Pi-Cation Pi-Cation Amide-Pi Pi-Alkyl

suggesting a potentially improved intracellular retention and bioavailability compared with the other molecules. Cytochrome P450 enzyme inhibition profiles were also examined to evaluate possible metabolic interactions. All derivatives were predicted to inhibit CYP1A2 and CYP2C19, indicating potential interactions with metabolic pathways involving these enzymes. Inhibition of CYP2C9 was observed in several compounds including MD-3, MD-4, MD-6, MD-7, MD-8, and MD-11, while CYP2D6 inhibition was predicted only for MD-3 and MD-11. Additionally, inhibition of CYP3A4, one of the most important drug-metabolizing enzymes, was predicted for MD-2, MD-3, MD-4, MD-6, MD-7, MD-8, MD-10, and MD-11. These findings suggest that some derivatives may have the potential to influence metabolic enzyme activity, which should be considered during further drug development. The skin permeability (log Kp) values ranged from –values ranged from, indicating moderate to low skin permeability among the compounds. Lower log Kp values correspond to reduced transdermal penetration, suggesting that the molecules are less likely to be absorbed through the skin. Overall, the pharmacokinetic evaluation demonstrates that most of the designed molecules possess favorable GI absorption and acceptable ADME characteristics, although their predicted interactions with cytochrome P450 enzymes and P-gp transporters may influence metabolic stability and drug-drug interactions. These findings provide valuable insight for selecting promising candidates for further molecular docking and biological activity studies.

Drug-Likeness Rule Evaluation of Designed Molecules

The drug-likeness of the Designed Molecules (MD-1 to MD-12) was evaluated using several widely accepted filters, including Lipinski, Ghose, Veber, Egan, and Muegge rules, along with the predicted bioavailability score given in Table 6. These rules help assess whether a compound possesses physicochemical properties consistent with successful orally active drugs.

According to Lipinski's rule of five, all molecules exhibited only one violation, which is generally considered acceptable for drug-like compounds. Lipinski's rule suggests that compounds with no more than one violation can still demonstrate good oral bioavailability. Therefore, the derivatives in this series maintain acceptable physicochemical characteristics for potential oral drug candidates. The Ghose filter analysis indicated that most compounds displayed one violation, while MD-7 and MD-11 showed two violations. Ghose criteria evaluate parameters such as molecular weight, molar refractivity, logP, and the number of atoms within the molecule. Although these two derivatives slightly exceed the recommended limits, the overall deviation remains relatively small and may not significantly affect their drug-likeness potential. Evaluation using the Veber rule, which focuses on rotatable bonds and Topological Polar Surface Area (TPSA), revealed no violations for any of the compounds. This suggests that all molecules possess favorable molecular flexibility and polarity, which are important factors for efficient oral absorption and membrane permeability. Similarly, the Egan filter, which predicts intestinal absorption based on TPSA and lipophilicity, showed one violation for all compounds. Despite this minor deviation, the values remain close to the acceptable limits, indicating that the derivatives still possess suitable characteristics for absorption. The Muegge drug-likeness rule also indicated one violation for each compound, suggesting minor deviations from ideal drug-like properties. However, compounds with a limited number of violations can still progress in drug discovery when supported by favorable biological activity. The bioavailability score for all molecules was predicted to be 0.55, indicating a moderate probability of achieving good oral bioavailability in humans. This consistent score across the series suggests that the designed derivatives share comparable pharmacokinetic potential. Overall, the drug-likeness assessment demonstrates that the designed molecules exhibit acceptable compliance with major drug-likeness filters, with only minor deviations observed in certain rules. These findings indicate that the compounds possess promising characteristics for further molecular docking studies, pharmacological evaluation, and lead optimization in drug development.

Molecular Docking Interaction Analysis

The molecular docking study was performed to evaluate the binding interactions between the designed ligand and the active site residues of the target protein given in Table 7. The graphical representation of molecular docking score was given in Figure 3. The three-dimensional docking pose illustrates that the ligand fits well within the binding pocket of the receptor, indicating a stable ligand-protein complex. The 3D interaction model (first image) demonstrates that the ligand is properly oriented inside the active site cavity and forms several stabilizing interactions with surrounding amino acid residues. Hydrogen bonding interactions play a crucial role in stabilizing the ligand within the binding pocket. These hydrogen bonds are typically formed between the electronegative atoms of the ligand and polar residues of the protein. In addition to hydrogen bonding, hydrophobic interactions and van der Waals contacts contribute significantly to the overall stability of the complex. Aromatic rings present in the ligand structure also facilitate π-π stacking and π-alkyl interactions with aromatic or hydrophobic residues of the receptor. The 2D interaction diagram (second image) provides a clearer representation of the specific amino acid residues involved in ligand binding. The ligand forms hydrogen bond interactions with residues such as SER and ARG, which may contribute to strong binding affinity. Furthermore, several hydrophobic residues including VAL, LEU, PRO, and ALA surround the ligand and form alkyl or π-alkyl interactions,

Table 4: Comparative Analysis of Physicochemical and Drug-Likeness Properties of Phenothiazine Structure interactions with #Rotatable bonds; #H-bond acceptors; #H-bond donors; MR; TPSA; iLOGP; XLOGP3.

Molecule	#Rotatable bonds	#H-bond acceptors	#H-bond donors	MR	TPSA	iLOGP	XLOGP3
MD-1	3	2	1	120.08	65.84	3.53	6.85
MD-2	3	1	0	118.06	45.61	3.78	6.65
MD-3	4	1	0	107.99	45.61	3.76	5.82
MD-4	4	2	0	124.55	54.84	4.08	6.62
MD-5	3	1	0	123.07	45.61	4.04	7.28
MD-6	4	3	0	122.03	65.69	3.41	6.48
MD-7	4	1	0	132.26	48.85	4.08	6.77
MD-8	4	2	0	123.44	62.68	3.53	6.11
MD-9	4	2	0	124.55	54.84	4.08	6.62
MD-10	3	1	0	123.07	45.61	4.04	7.28
MD-11	3	2	1	120.08	65.84	3.53	6.85
MD-12	4	3	0	122.03	65.69	3.41	6.48

Table 5: Comparative Analysis of Pharmacokinetic and ADME Properties.

Molecule	GI absorption	BBB permeant	Pgp substrate	CYP1A2 inhibitor	CYP2C19 inhibitor	CYP2C9 inhibitor	CYP2D6 inhibitor	CYP3A4 inhibitor	log Kp (cm/s)
MD-1	High	No	Yes	Yes	Yes	No	No	No	-3.85
MD-2	High	No	Yes	Yes	Yes	No	No	Yes	-3.89
MD-3	High	No	Yes	Yes	Yes	Yes	Yes	Yes	-4.28
MD-4	High	No	Yes	Yes	Yes	Yes	No	Yes	-4.11
MD-5	Low	No	Yes	Yes	Yes	No	No	No	-3.66
MD-6	High	No	No	Yes	Yes	Yes	No	Yes	-4.29
MD-7	High	No	Yes	Yes	Yes	Yes	No	Yes	-4.07
MD-8	High	No	No	Yes	Yes	Yes	No	Yes	-4.45
MD-9	High	No	Yes	Yes	Yes	No	No	No	-4.24
MD-10	High	No	Yes	Yes	Yes	No	No	Yes	-4.12
MD-11	High	No	Yes	Yes	Yes	Yes	Yes	Yes	-3.67
MD-12	Low	No	Yes	Yes	Yes	No	No	No	-3.61

helping stabilize the ligand within the hydrophobic region of the binding pocket. Additional residues such as GLU and TYR are involved in polar or electrostatic interactions that further enhance the binding stability. These interactions collectively indicate that the designed molecule demonstrates a favorable binding mode within the receptor active site. The presence of multiple stabilizing interactions suggests strong affinity between the ligand and the target protein, which may contribute to its potential biological activity. Overall, the docking results suggest that the ligand forms stable hydrogen bonding, hydrophobic, and π-interactions with key amino acid residues, indicating that the compound could act as a promising candidate for further in vitro and in vivo pharmacological evaluation.

Table 6: Molecular Docking score of design molecules.

Molecule	Docking Score
MD-1	-9.5
MD-2	-8.1
MD-3	-7.4
MD-4	-8.2
MD-5	-10
MD-6	-10.1
MD-7	-10.4
MD-8	-10.2
MD-9	-9.1
MD-10	-9.6
MD-11	-8.5
MD-12	-8.8

DISCUSSION

The present study employed an integrated computational approach to evaluate the drug-likeness, pharmacokinetic properties, and binding affinity of the Designed Molecules (MD-1 to MD-12). Modern drug discovery increasingly relies on in silico screening methods, as they enable rapid identification of promising lead compounds with favorable physicochemical and pharmacological characteristics while reducing the time and cost associated with experimental studies. In this work, several important parameters, including physicochemical descriptors, pharmacokinetic behavior, drug-likeness rules, and molecular docking interactions, were systematically analyzed to assess the potential of the designed molecules as drug candidates. The physicochemical properties of the molecules were first analyzed to determine whether they fall within the acceptable range for orally active drugs. The number of rotatable bonds (3-4) observed in the designed compounds indicates moderate molecular flexibility, which is beneficial for maintaining conformational adaptability during ligand-protein binding while still preserving structural stability. Excessive flexibility can negatively affect bioavailability; therefore, the values obtained in this study suggest a favorable balance between rigidity and flexibility. Hydrogen bonding plays an important role in determining molecular recognition and interaction with biological targets. The molecules analyzed in this study contained 0-1 hydrogen bond donors and 1-3 hydrogen bond acceptors, which falls within the acceptable range for drug-like molecules. These values suggest that the compounds possess sufficient capability to participate in hydrogen bonding interactions with amino acid residues in the receptor binding site. In addition, the Molar Refractivity (MR) values ranging between approximately 107 and 132 indicate appropriate molecular size and polarizability, which can contribute to stronger intermolecular interactions within the binding pocket. Another key parameter evaluated was the Topological Polar Surface Area (TPSA), which influences membrane permeability and absorption. The TPSA values of the designed molecules ranged from 45.61 Å² to 65.84 Å², well below the commonly accepted limit of 140 Å² for good

Table 7: Multiple interactions involving different amino acids; 2D and 3D structures by MD -MD12 molecules.

Code	2D Images	3D Images
MD-1	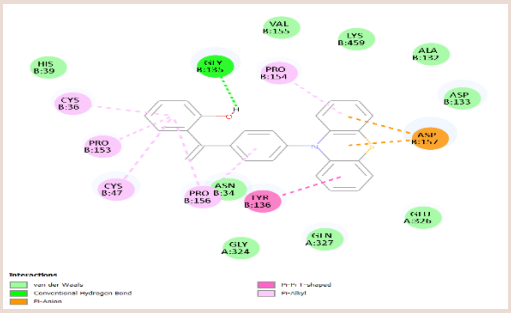	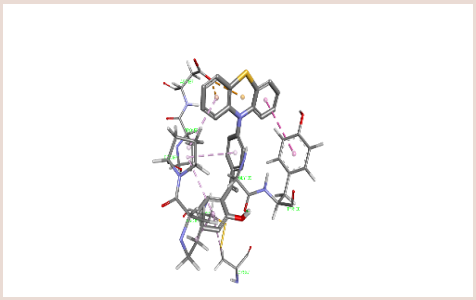
MD-2	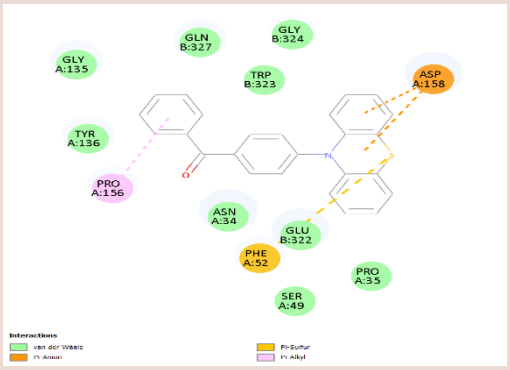	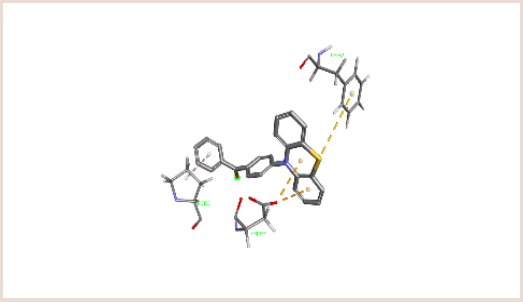
MD-3	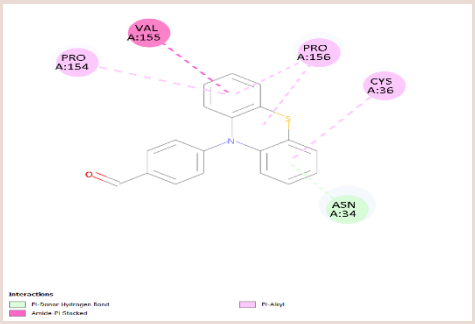	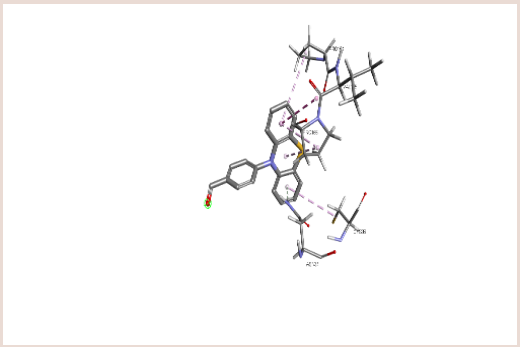
MD-4	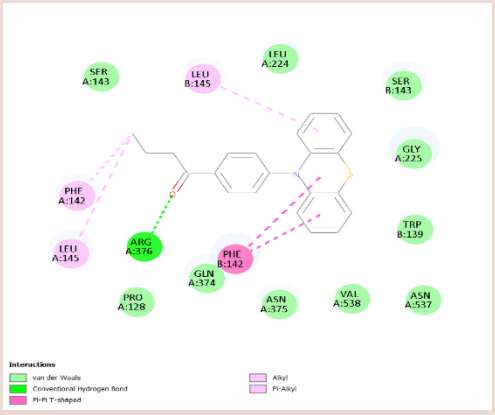	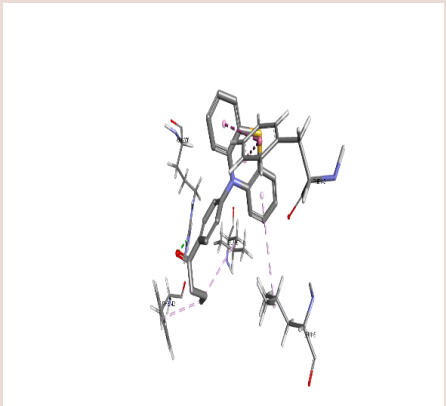

MD-5	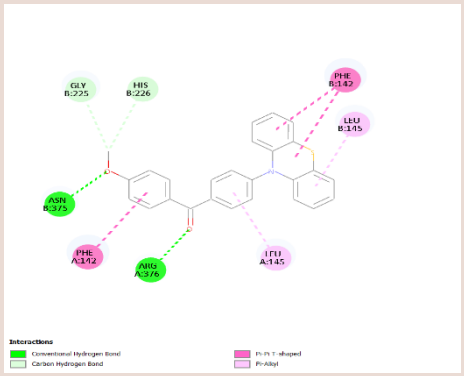	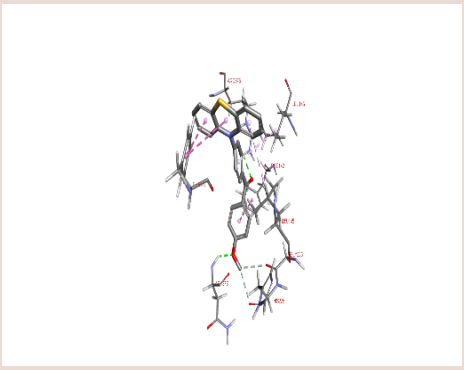
MD-6	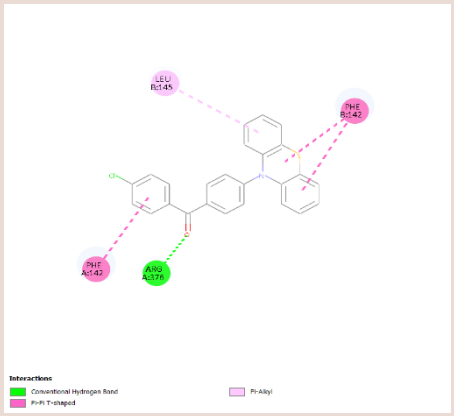	
MD-7	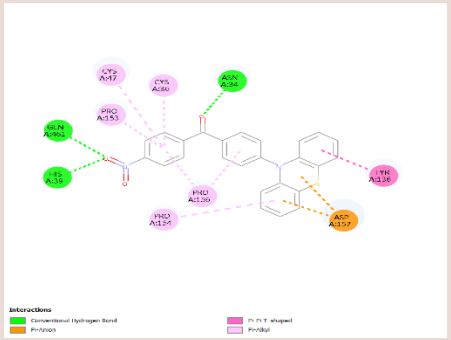	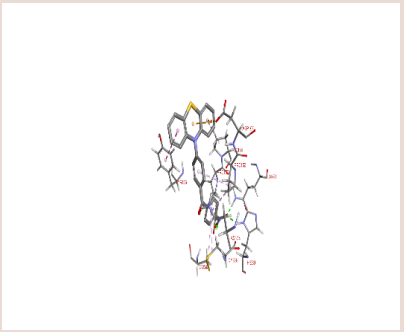
MD-8	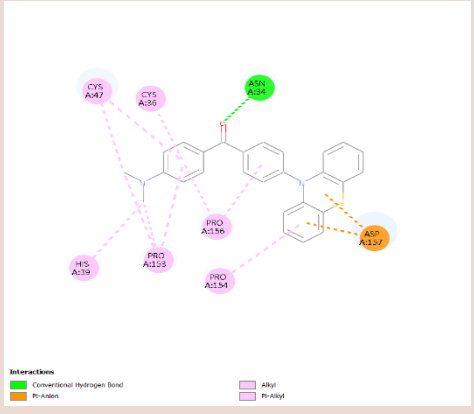	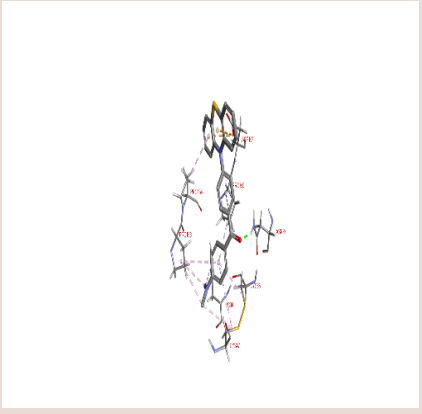

MD-9	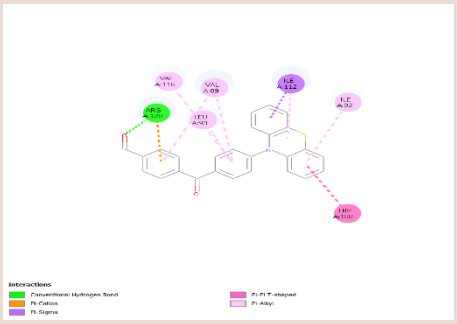	
MD-10	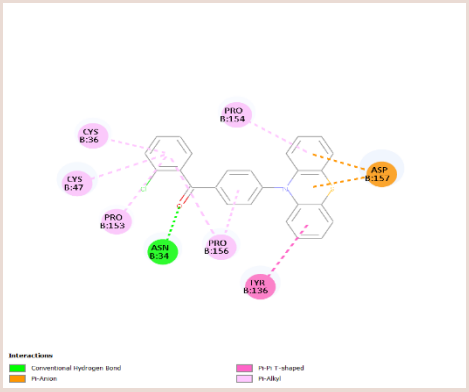	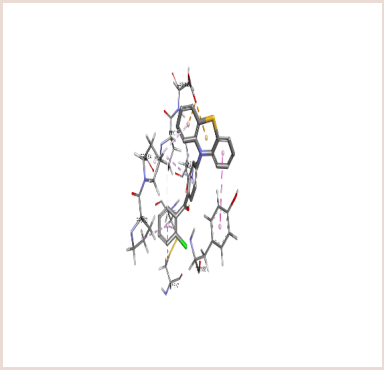
MD-11	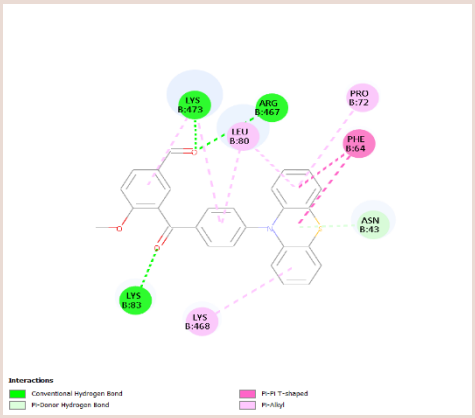	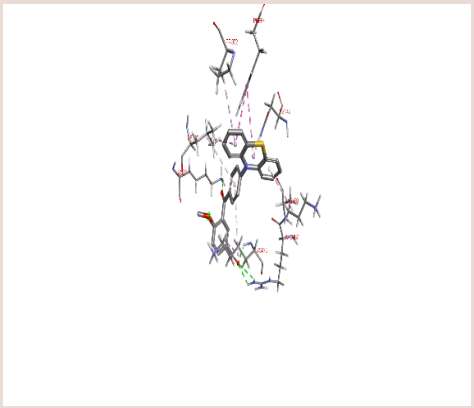
MD-12	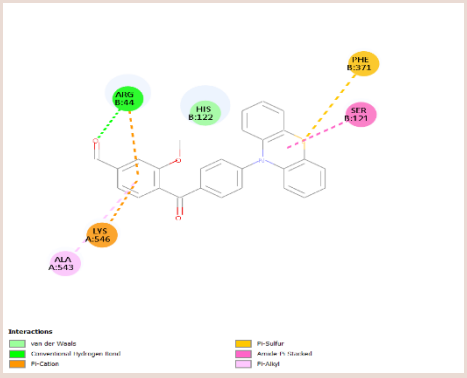	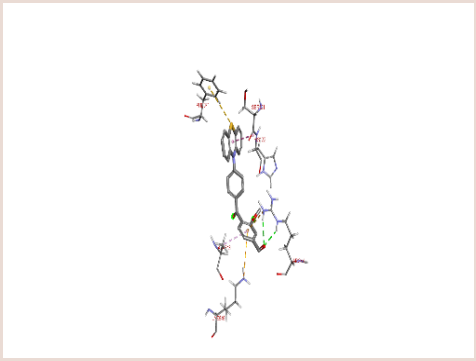

intestinal absorption. Such values indicate that the compounds possess suitable polarity for efficient passive diffusion across biological membranes. Compounds with TPSA values below 90 Å² are often associated with enhanced permeability, suggesting that the molecules in this series may demonstrate favorable absorption characteristics. Lipophilicity is also a critical determinant of drug absorption and distribution. The iLOGP values (3.41-4.08) and XLOGP3 values (5.82-7.28) obtained for the molecules indicate moderate lipophilicity. Adequate lipophilicity allows compounds to interact effectively with the hydrophobic environment of biological membranes and protein binding sites. However, excessively high lipophilicity may lead to poor solubility or metabolic instability. The values obtained in this study suggest that the molecules maintain a balanced hydrophilic-lipophilic profile, which is desirable for drug candidates. The pharmacokinetic properties predicted using ADME analysis further supported the drug-like nature of the designed compounds. Most molecules demonstrated high gastrointestinal absorption, indicating favorable oral bioavailability. Only two compounds, MD-5 and MD-12, showed relatively lower predicted GI absorption, suggesting that slight structural modifications could potentially improve their absorption characteristics. Additionally, none of the molecules were predicted to cross the blood-brain barrier, which may reduce the risk of central nervous system-related side effects when the therapeutic target is located outside the brain. Drug-likeness evaluation using multiple filters, including Lipinski, Ghose, Veber, Egan, and Muegge rules, indicated that the designed molecules largely satisfy the recommended criteria for orally active drugs. Each compound exhibited only one Lipinski violation, which is generally considered acceptable in drug discovery studies. Importantly, no violations Veber rule were observed in the, indicating favorable molecular flexibility and polarity for oral bioavailability. The predicted bioavailability score of 0.55 further suggests a moderate probability of good oral bioavailability. The molecular docking results provided further insights into the interaction of the designed molecules with the target protein. The docking scores ranged from –further suggests amol, indicating moderate to strong binding affinity. Among the evaluated compounds, MD-7, MD-8, MD-6, and MD-5 exhibited the most favorable docking scores, suggesting stronger interactions with the receptor active site. The docking interaction analysis revealed the presence of several stabilizing interactions, including hydrogen bonds, electrostatic interactions, salt bridges, π-π stacking, and hydrophobic interactions. These interactions are essential for stabilizing the ligand within the binding pocket and enhancing the binding affinity of the ligand-protein complex. Overall, the integrated computational analysis demonstrates that the designed molecules possess favorable physicochemical properties, acceptable pharmacokinetic behavior, and strong binding interactions with the target protein. In particular, compounds MD-5, MD-6, MD-7, and MD-8 emerged as the most promising candidates due to their strong docking scores and stable interaction patterns. These findings suggest that the identified molecules may serve as potential lead compounds and warrant further investigation through experimental biological assays and structure optimization studies.

CONCLUSION

In the present study, a series of twelve Designed Molecules (MD-1 to MD-12) were evaluated using comprehensive *in silico* approaches, including physicochemical property analysis, pharmacokinetic prediction, drug-likeness assessment, and molecular docking studies. These computational techniques are widely used in modern drug discovery to identify promising lead compounds before proceeding to experimental validation. The results obtained from the various analyses provided valuable insights into the potential biological and pharmacological properties of the designed molecules. The molecular docking analysis provided further evidence regarding the binding potential of the designed compounds with the target protein. The docking scores ranged from –provided, suggesting moderate to strong binding affinities. Among the tested molecules, MD-7, MD-8, MD-6, and MD-5 demonstrated the most favorable docking scores, indicating stronger interactions with the receptor active site. Detailed interaction analysis revealed that the compounds formed multiple stabilizing interactions, including hydrogen bonds, electrostatic interactions, salt bridges, π-π stacking, and hydrophobic interactions with key amino acid residues within the binding pocket. These interactions play a critical role in stabilizing the ligand-protein complex and enhancing binding affinity. Overall, the integrated computational results suggest that the designed molecules possess favorable physicochemical characteristics, promising pharmacokinetic properties, and strong binding interactions with the target protein. Among the evaluated compounds, MD-5, MD-6, MD-7, and MD-8 emerged as the most promising candidates based on their docking performance and acceptable drug-likeness profiles. Therefore, these compounds may serve as potential lead molecules for further *in vitro* and *in vivo* biological studies, as well as structural optimization, to validate their therapeutic potential and advance the drug development process.

ACKNOWLEDGEMENT

The authors are Thankful to Pravara Rural College of Pharmacy, Pravaranagar.

ABBREVIATIONS

ADME: Absorption, Distribution, Metabolism, and Excretion; **BBB:** Blood-Brain Barrier; **CNS:** Central Nervous System; **CYP:** Cytochrome P450; **CYP1A2:** Cytochrome P450 1A2; **CYP2C19:** Cytochrome P450 2C19; **CYP2C9:** Cytochrome P450 2C9; **CYP2D6:** Cytochrome P450 2D6; **CYP3A4:** Cytochrome P450 3A4; **GI:** Gastrointestinal; **HBA:** Hydrogen Bond Acceptor; HBD:

Hydrogen Bond Donor; **Log Kp:** Logarithm of Skin Permeation Coefficient; **LogP:** Logarithm of Octanol: Water Partition Coefficient; **MW:** Molecular Weight; **PSA:** Polar Surface Area; **SA Score:** Synthetic Accessibility Score.

CONFLICT OF INTEREST

The authors declare that there is no conflict of interest.

REFERENCES

Abraham, C., & Cho, J. H. (2009). Inflammatory bowel disease. New England Journal of Medicine, 361(21), 2066-2078. https://doi.org/10.1056/NEJMra0804647

Barnes, P. J. (2011). Pathophysiology of inflammatory bowel disease. Journal of Allergy and Clinical Immunology, 128(6), 1209-1217. https://doi.org/10.1016/j.jaci.2011.09.013

Baumgart, D. C., & Sandborn, W. J. (2012). Crohn's disease. The Lancet, 380(9853), 1590-1605. https://doi.org/10.1016/S0140-6736(12)60026-9

Chen, A. Y., & Liu, L. F. (1994). DNA topoisomerases: Essential enzymes and lethal targets. Annual Review of Pharmacology and Toxicology, 34, 191-218. https://doi.org/10.1146/annurev.pa.34.040194.001203

Daina, A., Michielin, O., & Zoete, V. (2017). SwissADME. Scientific Reports, 7, 42717. https://doi.org/10.1038/srep42717

Danese, S., & Fiocchi, C. (2011). Ulcerative colitis. New England Journal of Medicine, 365(18), 1713-1725. https://doi.org/10.1056/NEJMra1102942

DiMasi, J. A., Grabowski, H. G., & Hansen, R. W. (2016). Drug development cost. Journal of Health Economics, 47, 20-33. https://doi.org/10.1016/j.jhealeco.2016.01.012

Egan, W. J., Merz, K. M., & Baldwin, J. J. (2000). Prediction of drug absorption. Journal of Medicinal Chemistry, 43(21), 3867-3877. https://doi.org/10.1021/jm000292e

Ghose, A. K., Viswanadhan, V. N., & Wendoloski, J. J. (1999). Drug-like database design. Journal of Combinatorial Chemistry, 1(1), 55-68. https://doi.org/10.1021/cc9800071

Kaplan, G. G. (2015). The global burden of IBD. The Lancet, 385(9979), 1798-1800. https://doi.org/10.1016/S0140-6736(14)61998-9

Kitchen, D. B., Decornez, H., Furr, J. R., & Bajorath, J. (2004). Docking and scoring. Nature Reviews Drug Discovery, 3(11), 935-949. https://doi.org/10.1038/nrd1549

Lionta, E., Spyrou, G., Vassilatis, D. K., & Cournia, Z. (2014). Docking in drug discovery. Current Topics in Medicinal Chemistry, 14(16), 1923-1938. https://doi.org/10.2174/1568026614666140929124445

Lipinski, C. A. (2004). Rule of five. Drug Discovery Today: Technologies, 1(4), 337-341. https://doi.org/10.1016/j.ddtec.2004.11.007

Meng, X. Y., Zhang, H. X., Mezei, M., & Cui, M. (2011). Molecular docking overview. Current Computer-Aided Drug Design, 7(2), 146-157. https://doi.org/10.2174/157340911795677602

Morris, G. M., & Lim-Wilby, M. (2008). Molecular docking methods. Methods in Molecular Biology, 443, 365-382. https://doi.org/10.1007/978-1-59745-177-2_19

Muegge, I. (2003). Selection criteria for drug-like compounds. Journal of Medicinal Chemistry, 46(3), 254-261. https://doi.org/10.1021/jm020507e

Neurath, M. F. (2014). Cytokines in inflammatory bowel disease. Nature Reviews Immunology, 14(5), 329-342. https://doi.org/10.1038/nri3661

Pires, D. E., Blundell, T. L., & Ascher, D. B. (2015). pkCSM ADMET prediction. Journal of Medicinal Chemistry, 58(9), 4066-4072. https://doi.org/10.1021/acs.jmedchem.5b00104

Podolsky, D. K. (2002). Inflammatory bowel disease. New England Journal of Medicine, 347(6), 417-429. https://doi.org/10.1056/NEJMra020831

Pushpakom, S., et al. (2019). Drug repurposing. Nature Reviews Drug Discovery, 18(1), 41-58. https://doi.org/10.1038/nrd.2018.168

Ricciotti, E., & FitzGerald, G. A. (2011). Prostaglandins and inflammation. Arteriosclerosis, Thrombosis, and Vascular Biology, 31(5), 986-1000. https://doi.org/10.1161/ATVBAHA.110.207449

Sliwoski, G., Kothiwale, S., Meiler, J., & Lowe, E. W. (2014). Computational drug discovery. Pharmacological Reviews, 66(1), 334-395. https://doi.org/10.1124/pr.112.007336

Torres, J., Mehandru, S., Colombel, J. F., & Peyrin-Biroulet, L. (2017). Crohn's disease. The Lancet, 389(10080), 1741-1755. https://doi.org/10.1016/S0140-6736(16)31711-1

Trott, O., & Olson, A. J. (2010). AutoDock Vina. Journal of Computational Chemistry, 31(2), 455-461. https://doi.org/10.1002/jcc.21334

Vane, J. R., & Botting, R. M. (1998). COX inhibitors mechanism. Annual Review of Pharmacology and Toxicology, 38, 97-120. https://doi.org/10.1146/annurev.pharmtox.38.1.97

Veber, D. F., Johnson, S. R., Cheng, H. Y., Smith, B. R., Ward, K. W., & Kopple, K. D. (2002). Molecular properties. Journal of Medicinal Chemistry, 45(12), 2615-2623. https://doi.org/10.1021/jm020017n

Wallace, J. L. (2008). COX-2 in gastrointestinal injury. Gastroenterology, 134(2), 460-473. https://doi.org/10.1053/j.gastro.2007.11.017

Warner, T. D., & Mitchell, J. A. (2004). Cyclooxygenases. FASEB Journal, 18(7), 790-804. https://doi.org/10.1096/fj.03-0688rev

Wishart, D. S. (2016). DrugBank database. Nucleic Acids Research, 44(D1), D1074-D1082. https://doi.org/10.1093/nar/gkv1070

Xavier, R. J., & Podolsky, D. K. (2007). Unravelling IBD pathogenesis. Nature, 448(7152), 427-434. https://doi.org/10.1038/nature06005

Cite this article: Dharam MG, Bhor RJ, Kolhe MH, Bhoknal MR, Jadhav PS. *In silico* Design and Molecular Docking Evaluation of Phenothiazine Derivatives as Selective Celecoxib Bound to S121P Murine COX-2 Inhibitors for Targeted Therapy of Inflammatory Bowel Disease. Asian J Biol Life Sci. 2026;15(1):173-92.